Electronic Supplementary Material (ESI) for Analyst.

Supporting Information for:

Thin films of poly(vinylidene fluoride-*co*-hexafluoropropylene)-ionic liquid mixtures as amperometric gas sensing materials for oxygen and ammonia

Junqiao Lee, Ghulam Hussain, Nieves López-Salas, Douglas R. MacFarlane and Debbie S. Silvester

The Analyst

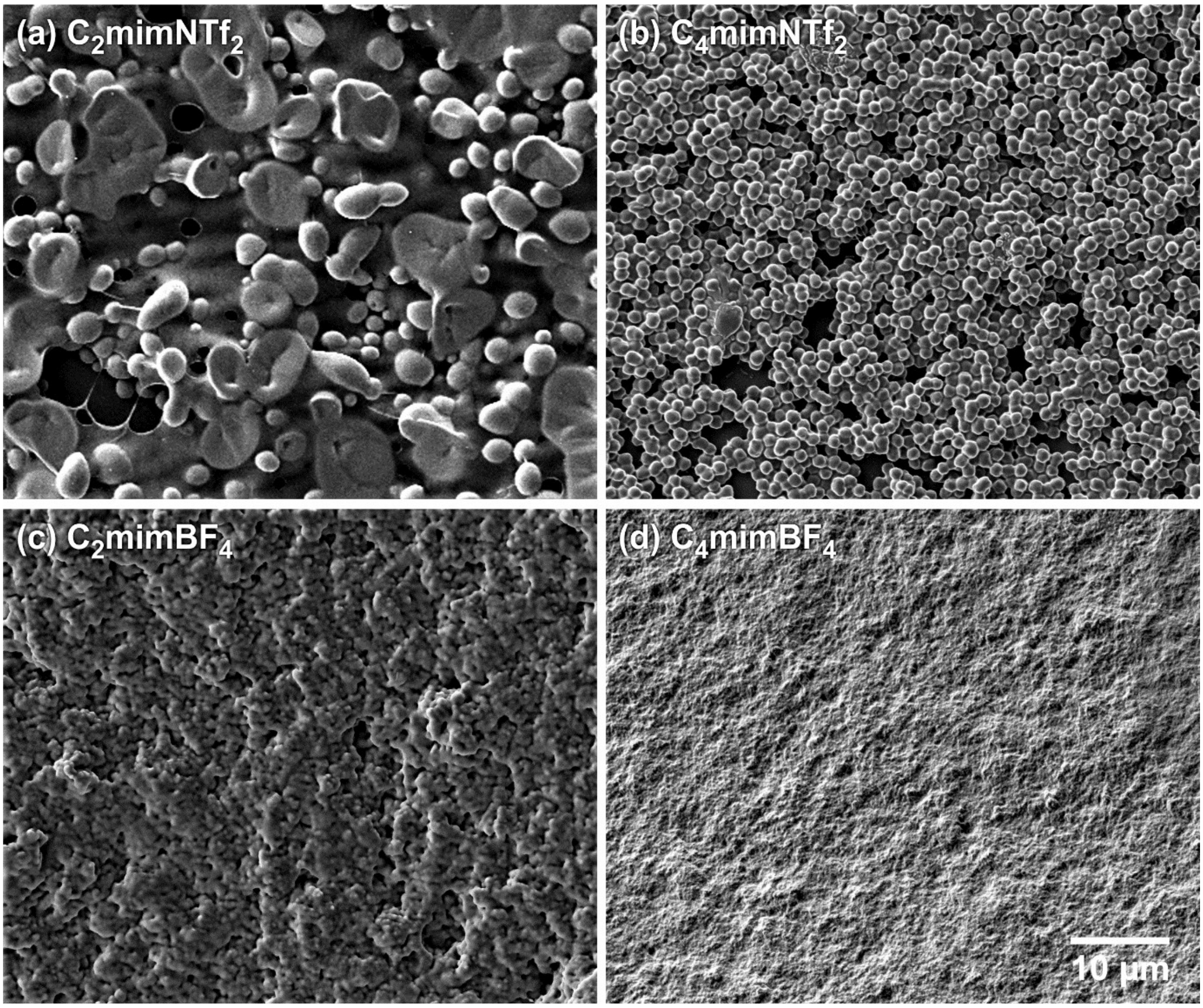

Figure S1. Scanning electron microscopy (SEM) images of: (a) [C_2mim][NTf_2]:PVDF-HFP, (b) [C_4mim][NTf_2]:PVDF-HFP, (c) [C_2mim][BF_4]:PVDF-HFP, and (d) [C_4mim][BF_4]:PVDF-HFP drop-casted films.

The images in Figure S1 show the very different structures formed by varying the RTIL cation and anion. There are significant differences simply by changing from the ethyl-substituted imidazolium cation ([C_2mim]$^+$) to the butyl-substituted imidazolium cation ([C_4mim]$^+$). Gradual deformation of the polymer “spheres” was observed during the SEM imaging as the result of exposure to the electron beam.

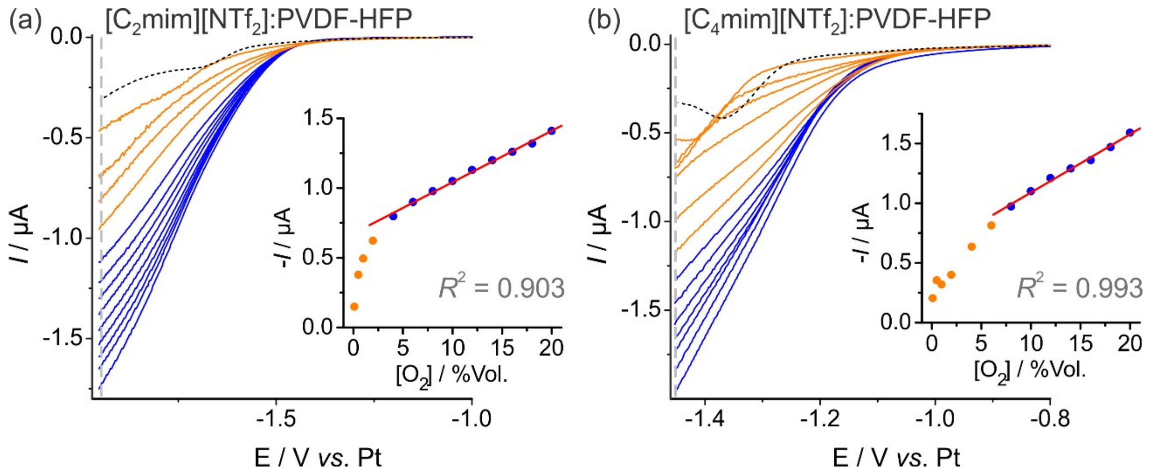

Figure S2. Linear sweep voltammetry (LSV) at a scan rate of 10 mVs^{-1} for O_2 reduction at 20, 18, 16, 14, 12, 10, 8, 6, 4, 2, 1, 0.5 and 0.1 % vol. O_2, using a 2:1 mass-ratio RTIL:PVDF-HFP gel-polymer electrolyte on a Pt TFE, with (a) [C_2mim][NTf_2] and (b) [C_4mim][NTf_2] as the RTIL. The black dashed lines are the responses in the absence of O_2. The insets show corresponding plots of background corrected currents (extracted at potentials indicated by the light grey vertical dashed lines) vs. % vol. [O_2], as well as the line of best fit within the linear range of each plot. The data points deviating from linear behaviour (orange) were not fitted.

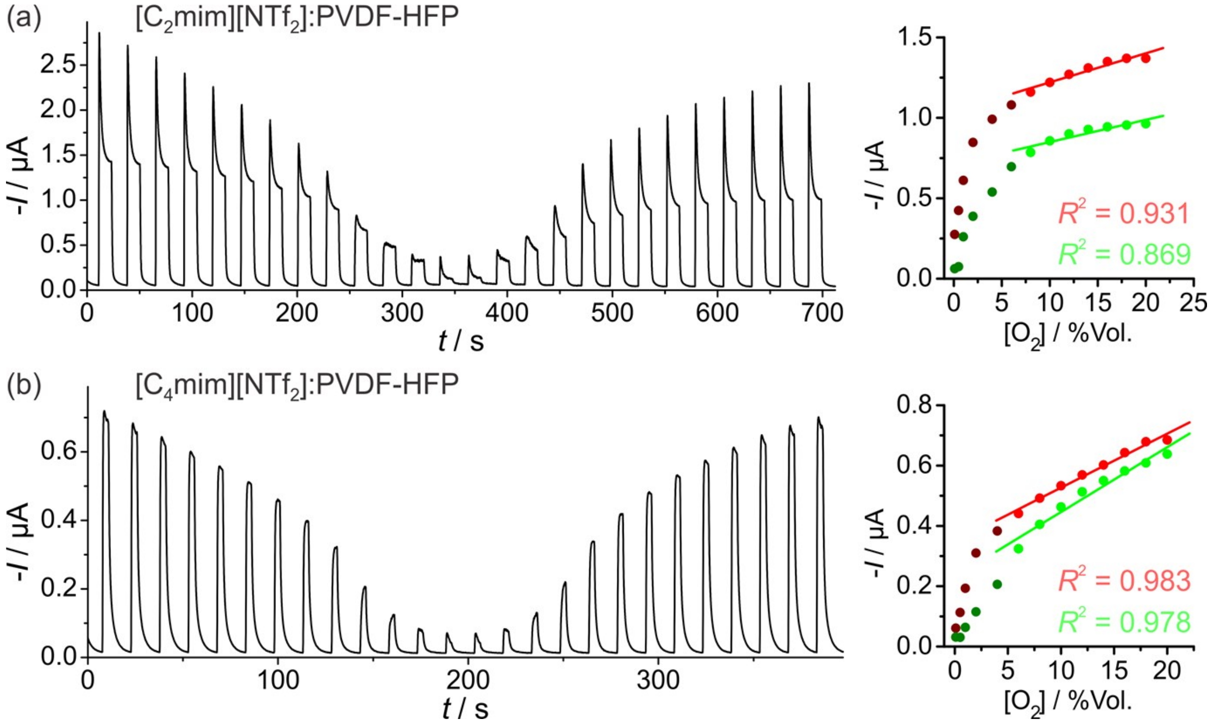

Figure S3. Long-term choronoamperometry (LTCA) for the reduction of 20, 18, 16, 14, 12, 10, 8, 6, 4, 2, 1, 0.5, 0.1 % vol. O_2 in a 2:1 mass-ratio RTIL:PVDF-HFP gel-polymer electrolyte on a Pt TFE, with (a) $[C_2mim][NTf_2]$, and (b) $[C_4mim][NTf_2]$ as the RTIL. A period of N_2 flushing between each concentration change was carried out to monitor the return of current to the baseline. The figures on the right-hand-side are the corresponding plots of background-corrected current vs. % vol. $[O_2]$, as well as the line-of-best-fit, for the descending (red) and ascending (green) phases. The current at the end of the transient (not the spike) was measured.

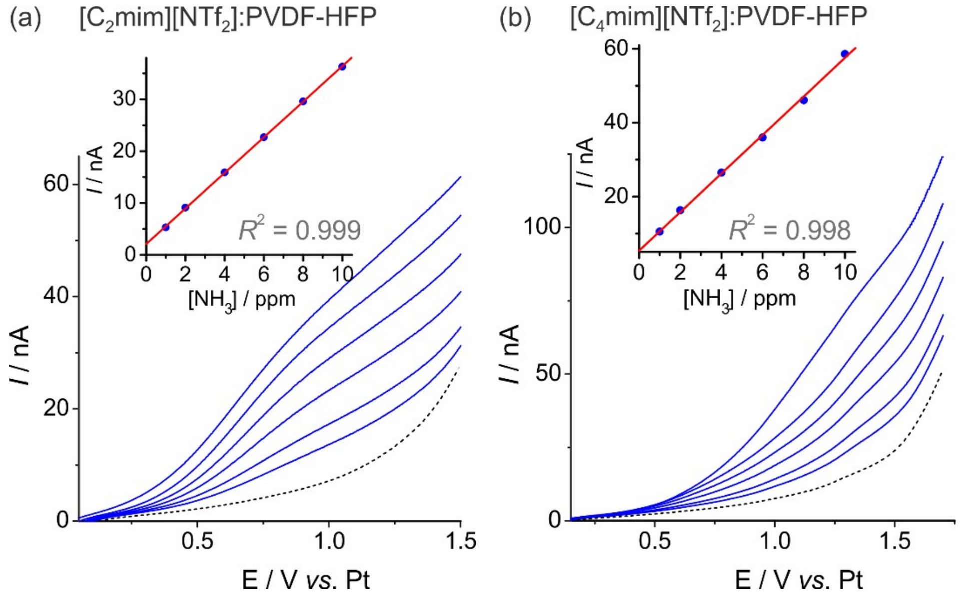

Figure S4. LSV for NH_3 oxidation at 10, 8, 6, 4, 2, 1 ppm of NH_3, in a 2:1 mass-ratio RTIL:PVDF-HFP gel-polymer electrolyte on a Pt TFE, with (a) $[C_2mim][NTf_2]$, and (b) $[C_4mim][NTf_2]$ as the RTIL, at a scan rate of 10 mVs^{-1}. The black dashed lines are the LSV responses in the absence of NH_3. The insets are corresponding plots of background corrected currents (extracted at potentials indicated by the light-grey vertical dashed lines) vs. different ppm concentrations of $[NH_3]$, as well as the line of best fit.

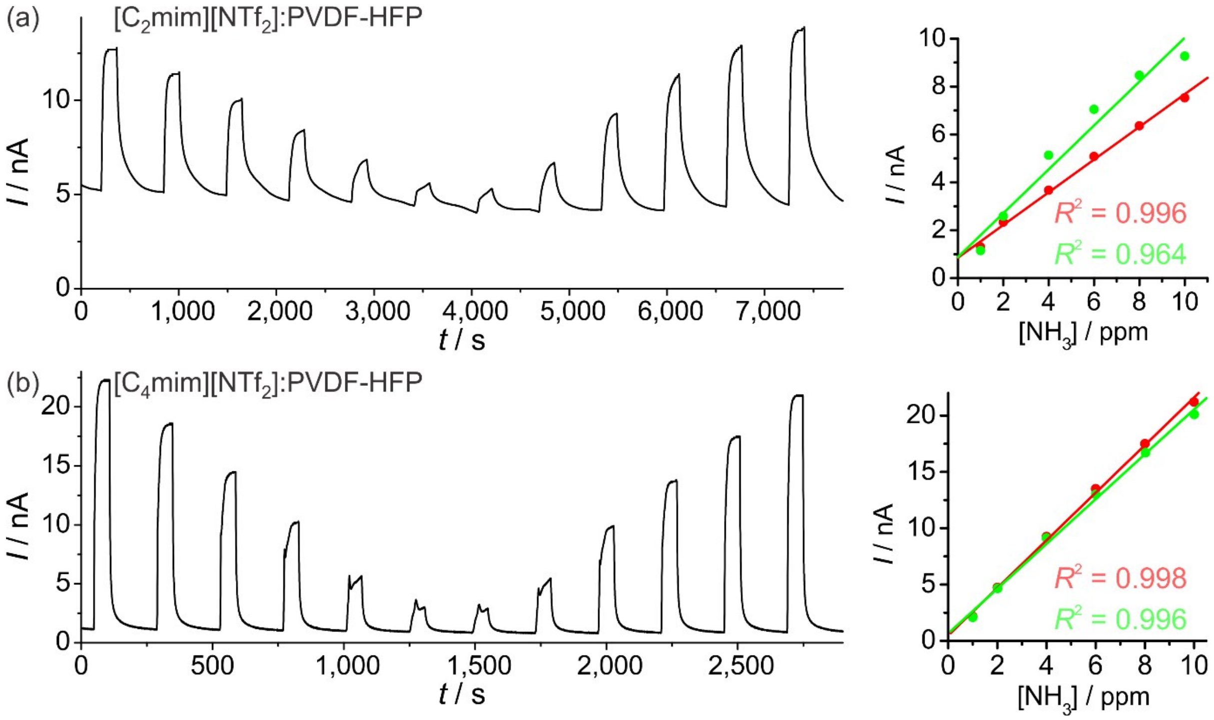

Figure S5. LTCA for the oxidation of NH_3 at (descending) 10, 8, 6, 4, 2, 1 ppm, and (ascending) 1, 2, 4, 6, 8, 10 ppm concentrations of NH_3, alternating with N_2 purging between each concentration change, in a 2:1 mass-ratio RTIL:PVDF-HFP gel-polymer electrolyte on a Pt TFE, with (a) $[C_2mim][NTf_2]$, and (b) $[C_4mim][NTf_2]$ as the RTIL. The figures on the right-hand-side are the corresponding plots of background corrected current vs. different ppm concentrations of $[NH_3]$, as well as the lines of best fit for the descending (red) and ascending (green) $[NH_3]$ phases.

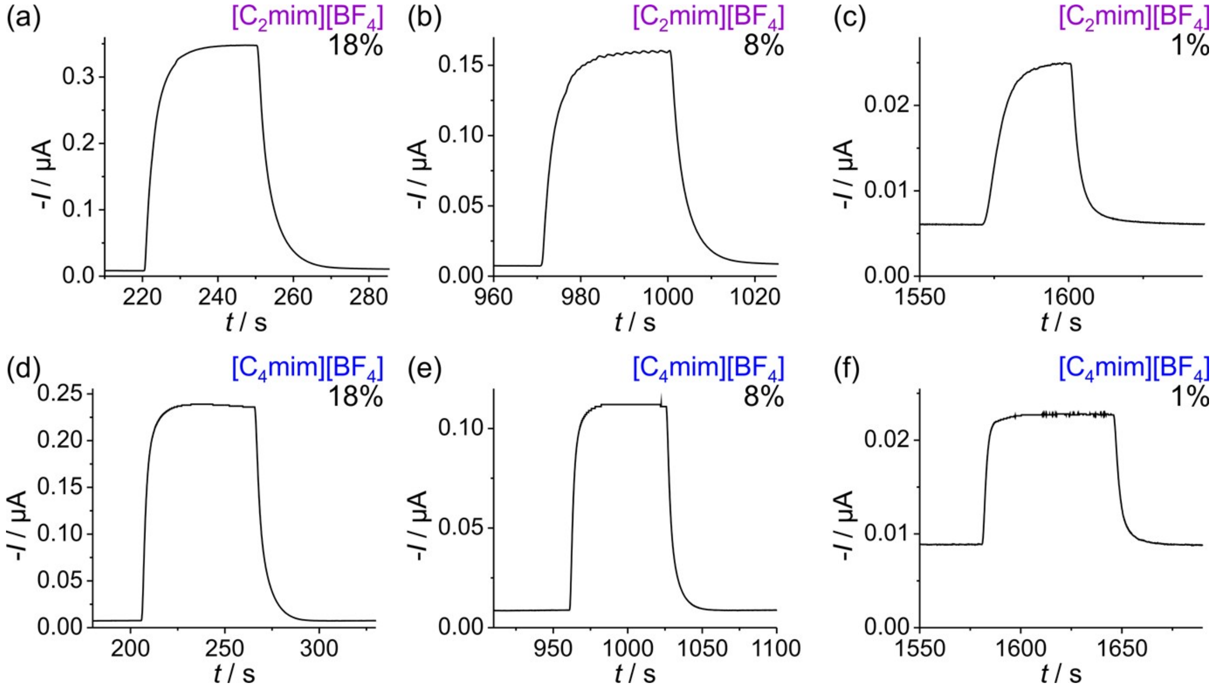

Figure S6. Close-up of selected current transients for oxygen sensing, taken from data in Figure 4 in the main text. The plots show the response and recovery cycles for 18 %, 8 % and 1 % O_2 on the descending current run.

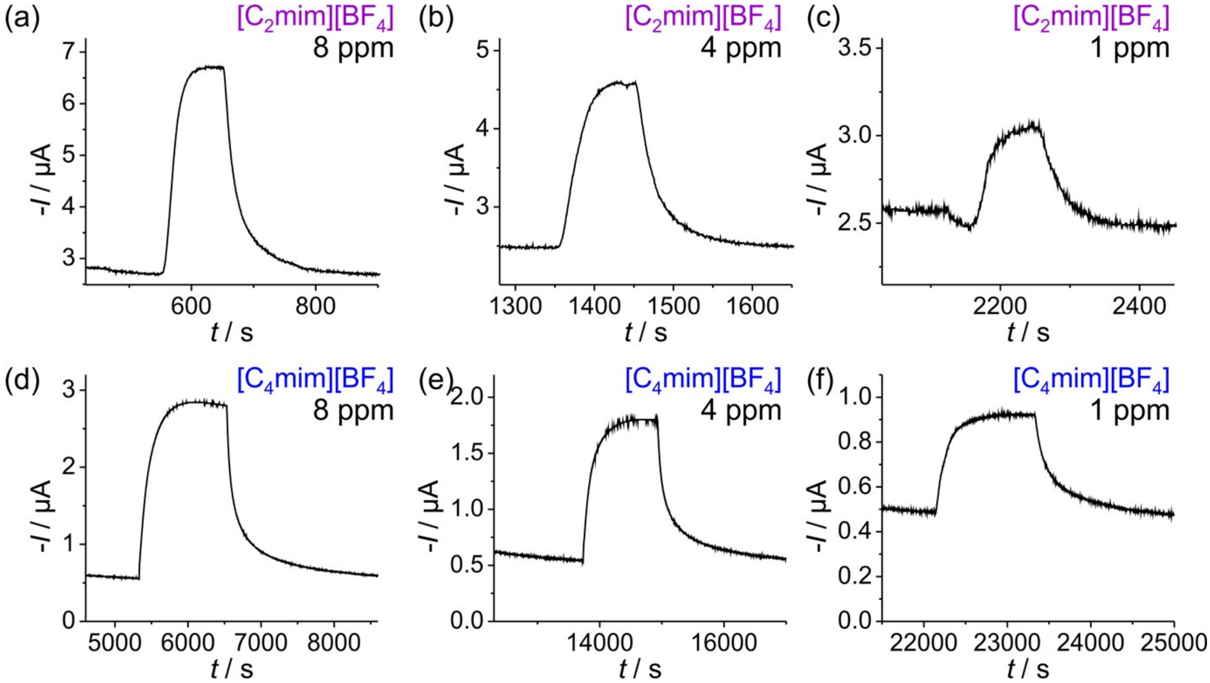

Figure S7. Close-up of selected current transients for ammonia sensing, taken from data in Figure 6 in the main text. The plots show the response and recovery cycles for 8, 4 and 1 ppm NH_3 on the descending current run.